Lawrence Berkeley National Laboratory

Title
Field test of a wideband downhole EM transmitter

Permalink
https://escholarship.org/uc/item/9qp5k63q

Author
Becker, Alex

Publication Date
1999-07-01

ERNEST ORLANDO LAWRENCE BERKELEY NATIONAL LABORATORY

Field Test of a WideBand Downhole EM Transmitter

Alex Becker, Ki Ha Lee, and Lou Reginato

Earth Sciences Division

July 1999

DISCLAIMER

Field Test of a WideBand Downhole EM Transmitter

Alex Becker, Ki Ha Lee, and Lou Reginato

Earth Sciences Division
Ernest Orlando Lawrence Berkeley National Laboratory
University of California
Berkeley, California 94720

July 1999

Field Test of a Wideband Downhole EM Transmitter

Alex Becker, Ki Ha Lee and Lou Reginato

Introduction

In a very striking numerical experiment, Lee and Xie (1993) demonstrated a technique for high resolution electromagnetic imaging of the subsurface by using the q-domain wavefield transform. Here, an electromagnetic current diffusion pattern was mathematically transformed to behave as a pseudo -sonic wavelet. The resultant pseudo-acoustic data were then successfully interpreted with a seismological ray-tracing technique. We were therefore encouraged to examine the practical feasibility of this methodology. As a first step in that direction, electromagnetic measurements were made on a laboratory scale model (Becker et al.,1994, Becker et al.,1997 and Das,1998).The results of these experiments confirmed that very precise crosswell em data can indeed be transformed to the wavefield domain. Additionally, we were able to define the signal bandwidth and signal strength specifications for a full- scale field system.

The next logical step in taking the q-transform technique from a numerical or a laboratory demonstration stage to implementation as a viable EM data interpretation method was to commence the fabrication of a full scale prototype system. In support of this objective, LBNL entered into a CRADA with Baker-Atlas (originally Western Atlas Logging Services, WALS). We were to be responsible for the theoretical and numerical work required for the field experiment design and data interpretation. Additionally, we undertook to fabricate the required downhole EM transmitter. WALS agreed to provide the downhole EM receiver ,the surface electronics , the wireline trucks, and to conduct the field work when the prototype equipment became available.

This report describes the design and construction of a prototype downhole EM transmitter and the results of a limited field experiment using a 100-m-deep well at the Richmond Field station operated by the University of California at Berkeley. The tests were principally designated to assess transmitter performance and were performed in a borehole to surface configuration with a commercially available receiver (Geonics EM 47) centered on the drillhole collar. Because of the short (30m or less) transmitter- receiver separations dictated by the logistics of the experiment and the relatively low ,50mS/m, conductivity of the intersected formations ,we realized that the recorded data would lack the bandwidth needed for its transformation to the wavefield domain(Becker et al.,1994). Consequently , transmitter performance was evaluated by comparing the observations with theoretical data that were corrected for the measured system response. Successful completion of these tests would assure the proper acquisition of data in a working cross-well environment where a 50m transmitter – receiver separation in a 300 mS/m formation would be used in conjunction with a high bandwidth receiver designed for this purpose.

General Design Overview

Our objective was to design, build and test a prototype time domain electromagnetic (TEM) transmitter specifically suited for subsurface use. The basic criterion for the design was the production of experimental data which could be used to assess the device

performance. We envisaged a simple self-contained ,modular transmitter design based on a long solenoid with a non-dissipative magnetic core. The switching electronics would be lodged in a second module and powered by batteries located in a third module. An overall tool length of about 6 m. and a weight of about 150 kg were deemed acceptable. A reference signal representative of the transmitter current waveform would be sent to the surface via an optic fiber link. These data are then used to synchronize and normalize the received signals. For the present tests the tool was lowered into the test hole via a nylon rope so that no electrical wires or other metallic conductors extended to the surface.
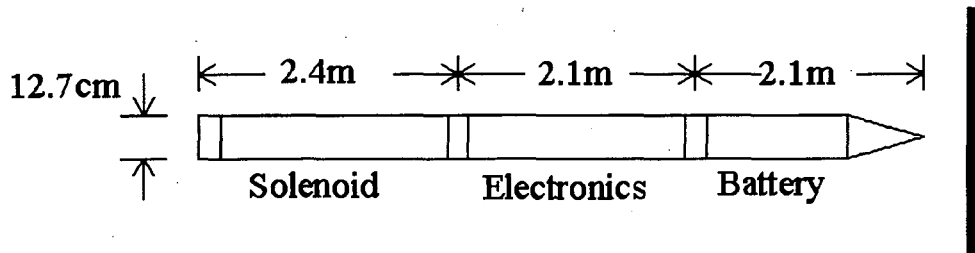

12.7cm

2.4m   2.1m   2.1m

Solenoid   Electronics   Battery

Figure 1   Tool Dimensions

Controlling Factors.

Ward and Hohmann (1989, Figures 2.4 and 2.5) show that the time domain impulse response , db/dt, of a dipole-dipole system within a homogeneous medium of conductivity σ can be characterized by a diffusion time t_0 given by

$$4t_0 = \mu \sigma r^2$$

Here, t_0 is in microseconds, σ in S/m and r is in meters. For a coaxial source- detector configuration , the maximum transient signal is observed at 0.4 t_0 microseconds after the extinction of the primary field. At that time, for a unit moment source in a non- magnetic environment , the maximum signal reaches a value of ;

$$db/dt = 0.6/\sigma \, r^2 \qquad V/m^2$$

One can conclude from the numerical results obtained by Lee and Xie (1993) that high fidelity time domain data located within a timespan defined by

$$t_0/10 < t < 10 t_0$$

are adequate for obtaining the proper wave domain response.Thus the diffusion time also sets the system bandwidth requirements. As shown by Das (1998) ,the transition time for the transmitter pulse from the "on" state to extinction should not exceed 5% of this quantity ,while the central frequency of a critically damped receiver should be greater than 15 times the reciprocal of the diffusion time.

The required transmitter moment is set by the desired signal-to-noise ratio at the peak signal time noting that the signal will fall by more than two orders of magnitude during the observation interval . Some preliminary tests at the Richmond test site, which is located in an industrial area and is strongly illuminated by a number of Bay Area AM radio stations, showed that the typical raw noise level ,at surface, was on the order of about 50 $\mu V/m^2$.

This value is believed to be a few orders of magnitude greater than the typical noise expected in a subsurface environment

To illustrate these concepts , let us look at the system requirements for the Richmond Field Station test with a 30m transmitter-receiver separation. In this case, assuming an average bedrock conductivity of 20 mS/m we have

$$t_0 = 5.6 \ \mu s$$

and the transient is to be observed in the interval,

$$0.6 < t < 60 \ \mu s \ .$$

The low diffusion time expected here precludes the distortionless observation of the transient signal .We would need to extinguish the transmitter current in less than one microsecond and observe the transient with a system bandwidth in excess of 2 Mhz. These conditions are much more stringent than those to be expected in a working environment where the diffusion times would be approximately ten times greater. Under these circumstances the peak observable signal should reach about $400nV/m^2$
for unit transmitter moment. Thus even with a modest transmitter moment of 100 A-m^2 we can expect to see a somewhat distorted signal throughout the observation timespan. While these estimates are made for the crosswell, coplanar coil configuration where the effect of the air-earth interface is ignored, numerical computations show that they are also valid for the surface-to-borehole measurements.

The Transmitter Solenoid

In order to optimize the transmitter moment we chose a solenoidal ferrite core construction. The core was made up of six solid cylindrical pieces of CMD 5005 material manufactured by Ceramic Magnetics Inc. They were held together by nylon stripping. Each piece was 3" in diameter and 1 foot long so that the solenoid had an overall length of 6'-0". To minimize flux loss, the faces on each piece were ground flat.

The core was wound with 27 widely spaced turns of #12 enamel covered wire. An electrostatic shield made of a thin copper tape was placed over the working winding. Care was taken to keep the shield winding open to avoid loading the transmitter with an effective shorted secondary turn. When completed, the solenoid had an inductance of 425 μH and a self-resonant frequency of 3.4 MHz. From this inductance value as well as a number of flux transformer (mutual inductance) data we were able to deduce that the relative permeability of the core was about $200 \pm 10\%$. Once demagnetization is accounted for, this value of relative permeability indicates either some flux leakage in the joints or a lower value of initial permeability than that indicated in the manufacturers literature. We would then expect the transmitter solenoid to have an effective area of about 25 m^2 and a magnetic moment of 250 A-m^2 when it carries a 10A current.

The Driver Electronics and Transmitter Performance

A synoptic schematic diagram for the driver which generates rectangular pulses of alternating polarity is shown in Figure 2. The desired waveform ,shown below in

Figure 3a originates in a conventional clock circuit. It is then used to control the A and B switchbanks. In order to generate the required sharp edge pulses, fast recovery insulated gate bipolar transistors (IGBT) were used. Five devices are connected in series and each is protected from overvoltage by an RC network and Zeners so that a maximum voltage of 5 kV can be tolerated when the magnetic dipole transmitter is switched off in one microsecond from a 10A current level. The ferrite loaded transmitter solenoid is driven by bipolar pulses to avoid any hysteresis in the magnetizing function and to compensate for any dc drift in the detector circuits. The IGBTs were chosen because of their high current, high voltage and fast turn-off switching speeds.The device was operated at a very low duty cycle using 5A, 1.1 ms square pulses of alternating polarity at a 66 pps rate and a waveform period of 33 ms. As shown in Figure 3b we have achieved a 10-90% fall time of 1.5 μs for the transmitted pulse. Because of the finite fall time, the pulse spectrum deviates from the ideal 1/f shape with an increase in spectral amplitude below 20 kHz and some attenuation above 200 kHz.

System Response

The total system response is equally defined by the receiver and the transmitter characteristics. It is best determined experimentally by putting the receiver in very close coupling with the transmitter so that any ground production effects are minimized. The impulse response for our system which consists of the transmitter under test and the commercial EM47 receiver is shown in Figure 4a. It represents the function with which one must convolve the ideally observable time derivative of the ambient magnetic field in order to predict the actual output of the receiver. The Fourier transform of the system impulse response is shown in Figure 4b. It simply represents the product of the transmitter pulse spectrum and the spectral response function of the EM47 receiver. The latter has a sensitivity that is directly proportional to frequency up to its resonance about 300 kHz. When this response function is combined with the approximate 1/f spectrum of the pulse we observe the low pass system response which attenuates all signal above this frequency .

The effects of finite system bandwidth can be readily demonstrated. Let us examine the expected signal distortion for some data records for the Richmond Field Station(RFS). The transmitter and receiver are coaxial with the receiver located on surface directly above the transmitter which is down hole. Electrical logs for RFS show that the resistivity of the unconsolidated surficial material traversed by the borehole is about 20 ohm-m. The results of the numerical simulation are shown in Figure 5. Severe signal distortion due to bandwidth limiting is observed in the data shown in Figure 5a where the transmitter is 10m below the receiver. Increasing this distance to 20 m, as is done for the data in Figure 5b, results in a signal with lower frequency content and an attendant reduction in distortion. Here the observable filtered signal strongly resembles the desired wideband signal in shape and size but is delayed by the system by about 1 microsecond. As the source is lowered below 40m, the system delay of the true signal becomes negligible.

Data Acquisition

Data acquisition was done with the Tektronix model TDS744A digital oscilloscope and was synchronous with the transmitter pulse. Because current pulses of opposing polarity are not identical, only signals related to the positive-to-zero current transition were recorded. Nine hundred pulses were averaged to produce the raw recorded signal which was sampled at 100 ns intervals. A typical ground response transient is shown in Figure 6. It is immediately apparent that the raw stacked data are offset both in time and in baseline voltage level and must be corrected for these effects. These corrections were applied in an empirical manner. The dc baseline shift was removed by adjusting the data level, prior to

4

the transient onset, to zero. The timing error in position of the transient onset is related to the near impossibility of finding the correct trigger position on the current waveform which is used to synchronize the data acquisition. Perhaps better results could have been obtained by using the transmitter clocking pulse instead of the band-limited current waveform for this purpose. Under the present circumstances, however, good correlation with theoretical data was obtained by setting the time axis zero just ahead of the intersection of the transient edge and the baseline. Finally, the observed data were averaged over a variable width time window. As described by Bentley (1993) one can easily improve the signal to noise ratio, especially at late observation times where the signal is small, by using this type of filter. The signal remains undistorted if the window width is proportional to the time of observation. In our case we used an 8% window. The effects of data processing on the raw observations are shown in Figure 6. The effects of baseline and time shifts are readily evident while the effect of the window filter on the data is less apparent. This is so because of the small linear scale. In fact, at late observation times the signal to noise ratio is improved by at least 10 dB.

Signal Fidelity

In order to verify the proper functioning of the entire system we compare the observations with their theoretical values. The latter were computed by taking the ideal impulse response for the RFS electrical section and convolving it with the system response shown in Figure 4a. The comparison is made in Figure 7 where data for a 15m and a 20m transmitter-receiver are shown. A reasonably good overall fit exists between the theoretical and the experimental data. In both cases, however, the experimentally observed pulses are somewhat wider than the computed ones. It also appears that the experimental pulse precedes its theoretical prediction, but this is an artifact caused by an improper shift of the time axis for the experimental data.

Transmitter Moment

The direct measurement of the magnetic moment of a large solenoidal transmitter is virtually impossible. If we use a close-coupled sensor some flux loss is inevitable. The use of a distant calibrated sensor usually implies the inclusion of some ground effects and possible stray coupling between the transmitter and receiver. As outlined by Tseng et al. (1998), the best procedure for transmitter calibration is a test where transmitter-receiver separation is varied. In our case, we compared the peak value of the observed formation transient and the peak value of the theoretical impulse response after it was convolved with the system function. This was done for a number of separation values between the vertical axis sensor at surface and the borehole transmitter. Since the theoretical values were computed for a unit transmitter moment, the common factor by which the experimental values once normalized by the transmitter current have to be divided to obtain a best fit between the two data sets represents the product of the effective areas of transmitter and receiver. The comparison of our observations with the corresponding theoretical data is shown in Figure 8 where both data sets fall inversely as the 9/2 power of the distance between receiver and transmitter. A common dividend of 3300 was used to superpose the observed data (normalized by the transmitter current) on the theoretical results. Allowing for the 31.4 m^2 effective area of the receiver, we find that for a current of 5A, the transmitter to have a moment of 105A-m^2 and an effective area of 21 m^2. If we now take into account the 27 turn winding and the 4.6 x 10^{-3} m^2 physical area of cross section of the ferrite core we find the relative magnetic permeability of the core to be about 170. This value is not much lower than expected and is probably related to leakage in the core joints

5

that develops with use. Thus at the standard 5A current ,the transmitter had a moment of 105 A-m^2.

Conclusions and Discussion

A viable large bandwidth TEM transmitter can be constructed using very conventional means although in the present case the effective magnetic permeability of the solenoid core was lower than expected. Only a small number of turns can be used to maintain reasonably low inductance. This has to be compensated with the use of large currents. In this case, good ventilation must be provided to avoid overheating the electronics. In our case the most temperature sensitive element was the optic fiber transmitter which usually failed after about an hour of operation. Care must also be taken to guarantee balance between the negative and positive pulses as this improves the signal/noise ratio. Finally, we reiterate the need to review the origin and nature of the trigger pulse so that consistent properly clocked data can be acquired. In spite of the limited nature of the RFS tests which prevented us from acquiring data suitable for a direct demonstration of the wavefield transform, we did secure high quality wideband data that confirmed the proper performance of the prototype transmitter. We are certain that this equipment can now be used in an oil-field environment to acquire data suitable for a practical verification of the wavefield transform.

Acknowledgments

References

Becker, A., Lee, K. H., Wang, Z., and Xie, G., 1994, Acquisition of precise electromagnetic data: EAEG 56th Annual Meeting and Exhibition/6th EAPG Conference, Vienna, Austria, June 6-10.
Becker, A., Das, K. K., and Lee, K. H.,1997, Validation of the EM wavefield transform: 59th EAGE Annual Conference and Exhibition, Geneva, Switzerland, May 26-30.
Bently, R., 1993, Time domain EM scale model, M.S. Thesis, Materials Science and Mineral Engineering, University of California at Berkeley.
Das, K., 1996, Experimental validation of the wavefield transform, M.S. Thesis, Materials Science and Mineral Engineering,University of California at Berkeley.
Lee, K. H., and Xie, G., 1993, A new approach to imaging with low-frequency electromagnetic fields, Geophysics, 58, 780-796.

DIPOLE MAGNET SWITCHER PULSER PROBE

SWITCHER CLOCK

SWITCHER DRIVER BANK A	SWITCHER DRIVER BANK B

+100V

A

B

IGBT A & B SWITCHER BANKS

+100 V IN

A

B

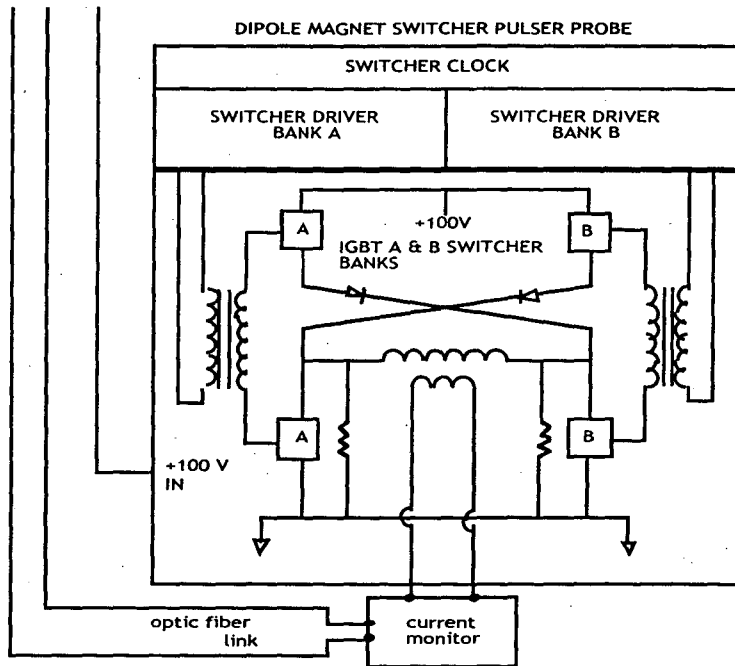optic fiber link

current monitor
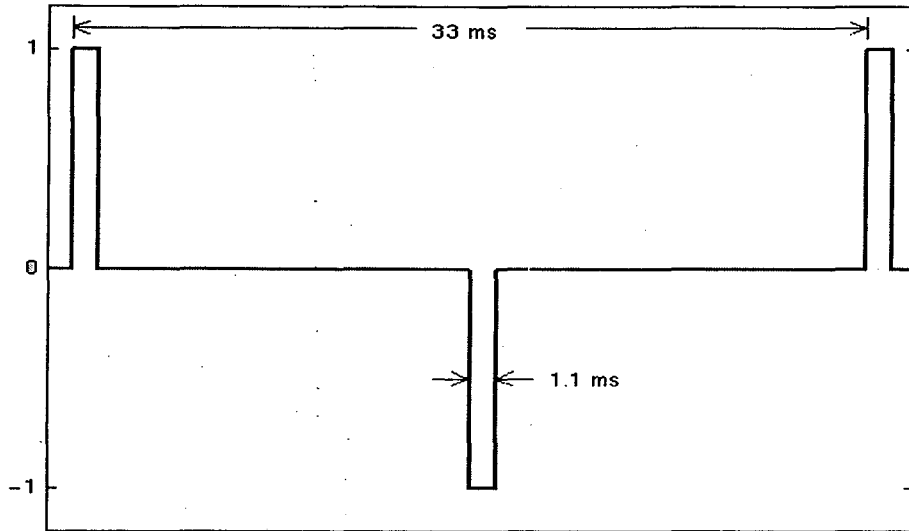
Figure 2 – Driver schematic
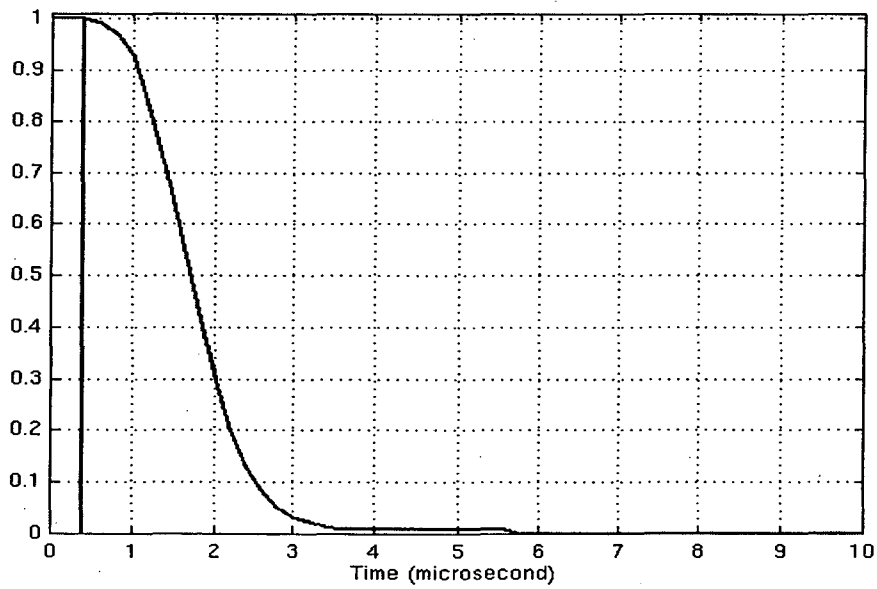
Figure 3a – Current waveform
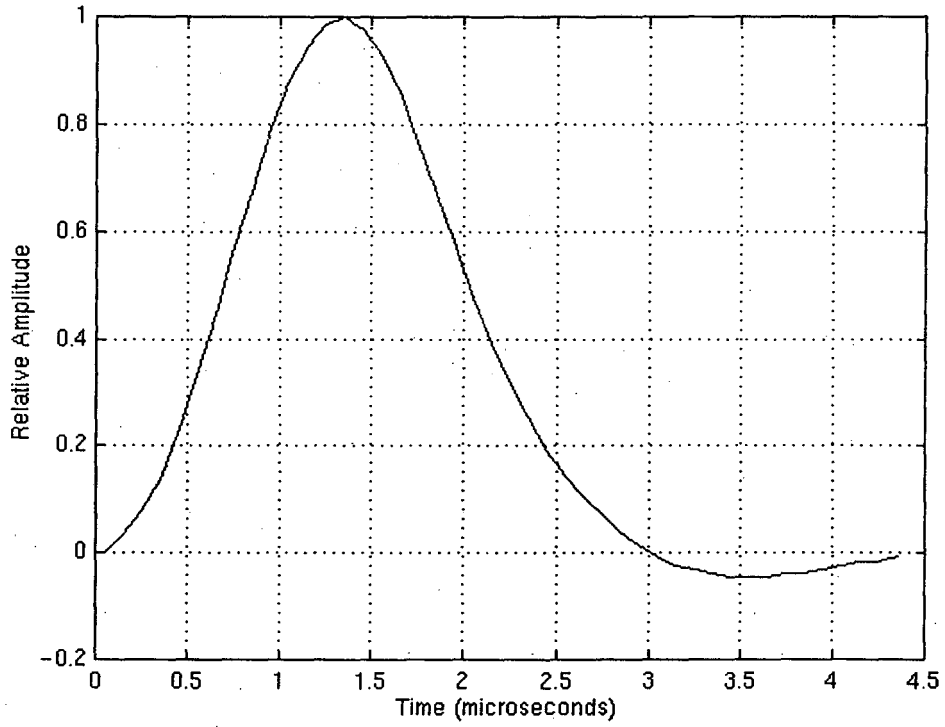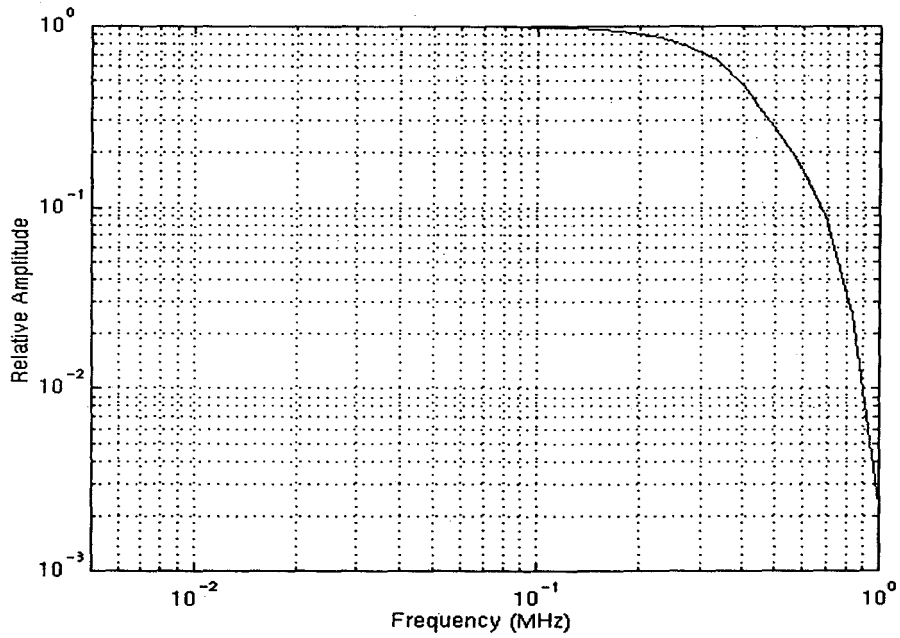

Figure 3b – Pulse transient

Figure 4a – System step response

Figure 4b – System transfer function
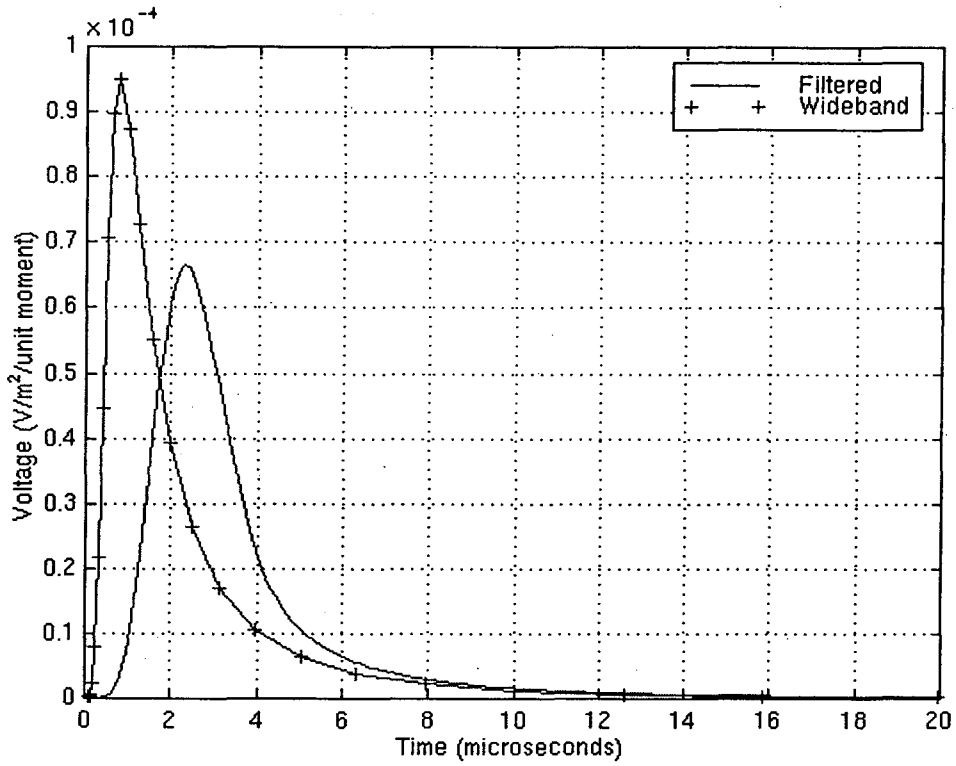
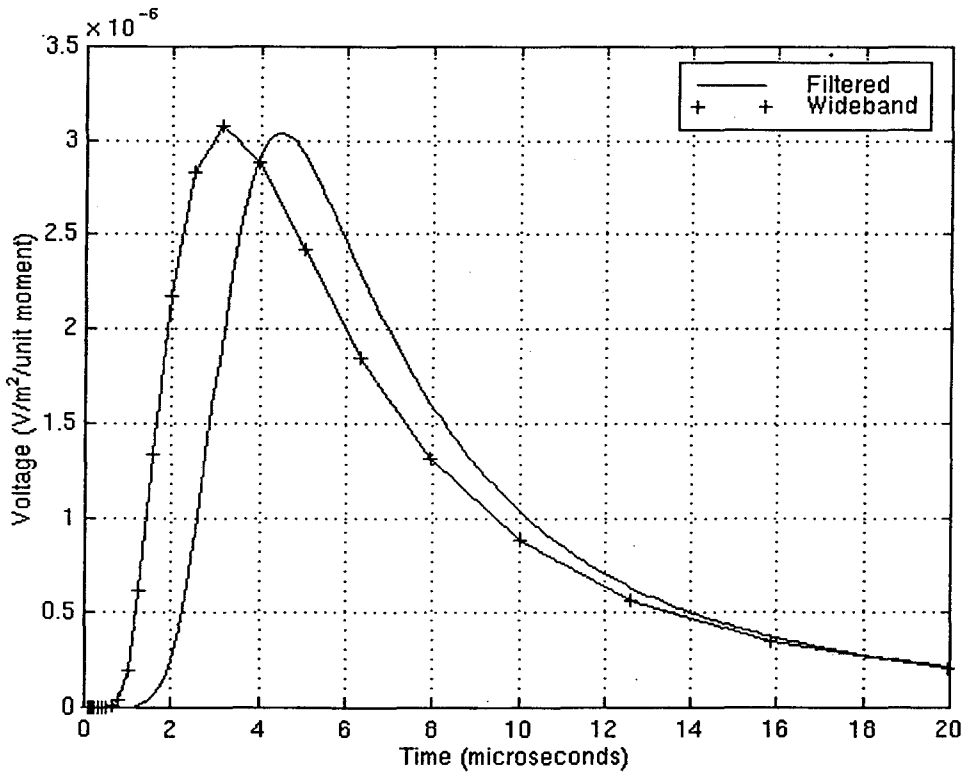Figure 5a – System simulation with the transmitter at 10m depth
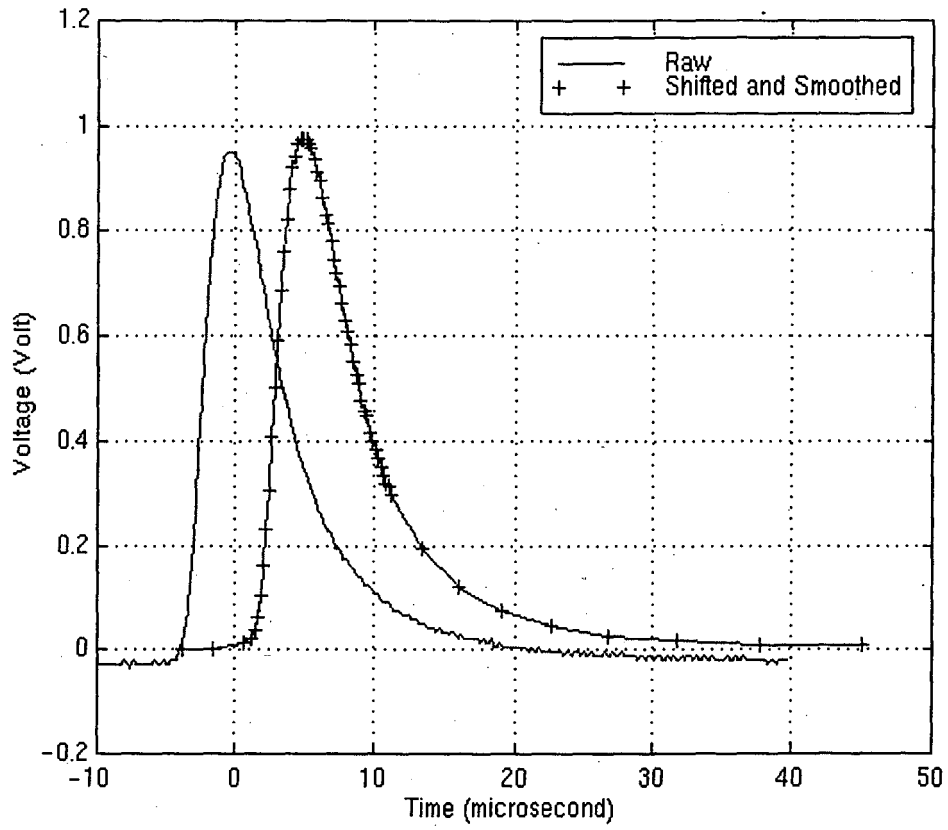

Figure 5b – System simulation with the transmitter at 20m depth
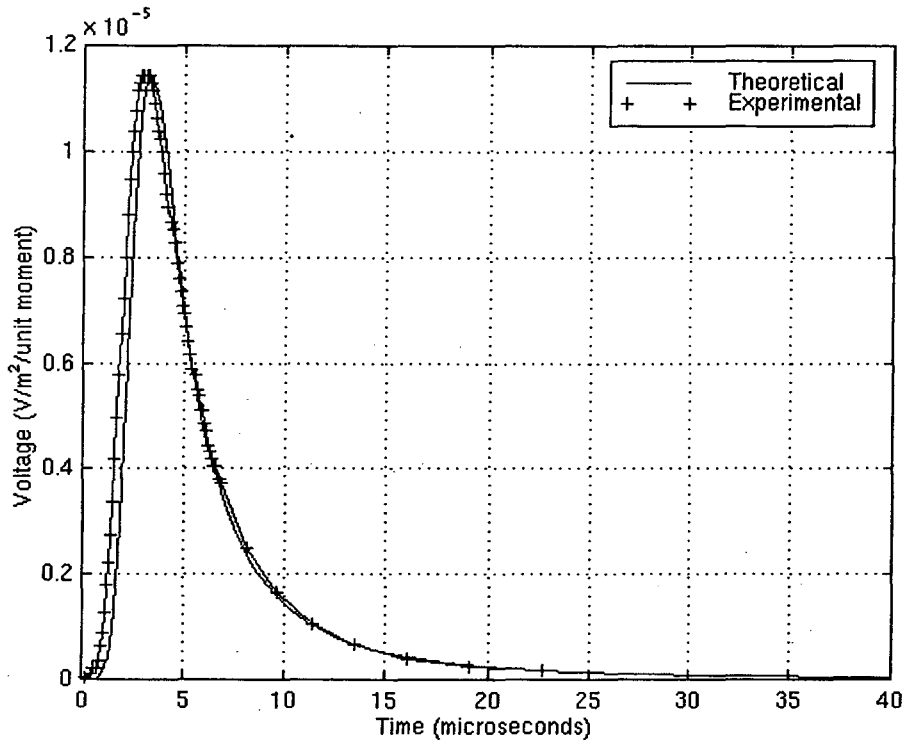
Figure 6 – Effects of data processing

Figure 7a – Comparison of experimental data with theoretical prediction
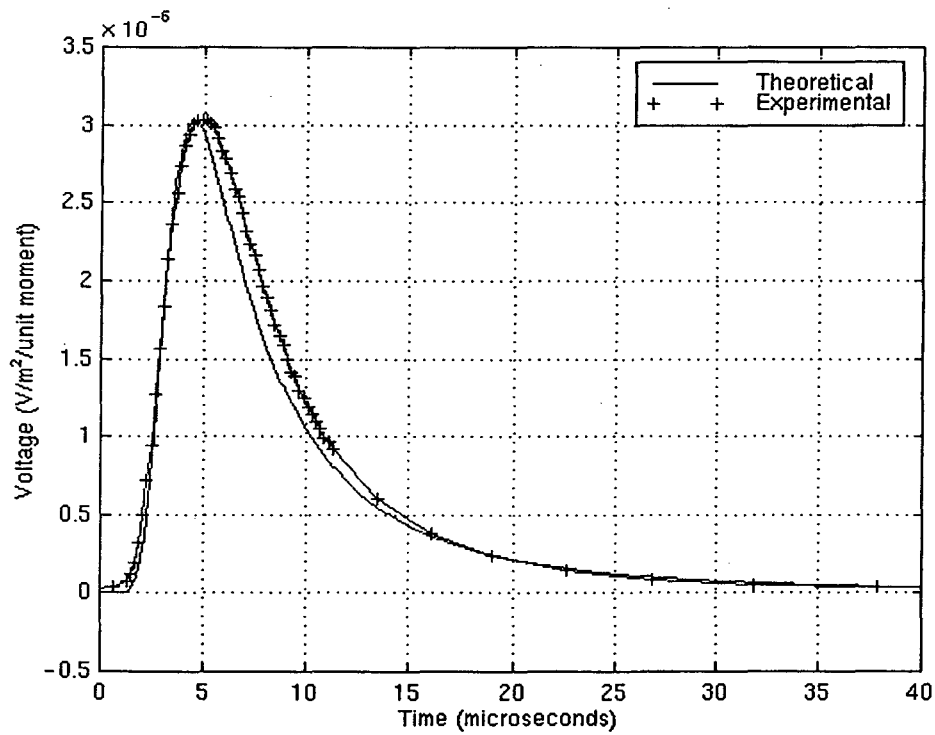Transmitter at 15m

Figure 7b – Comparison of experimental data with theoretical prediction
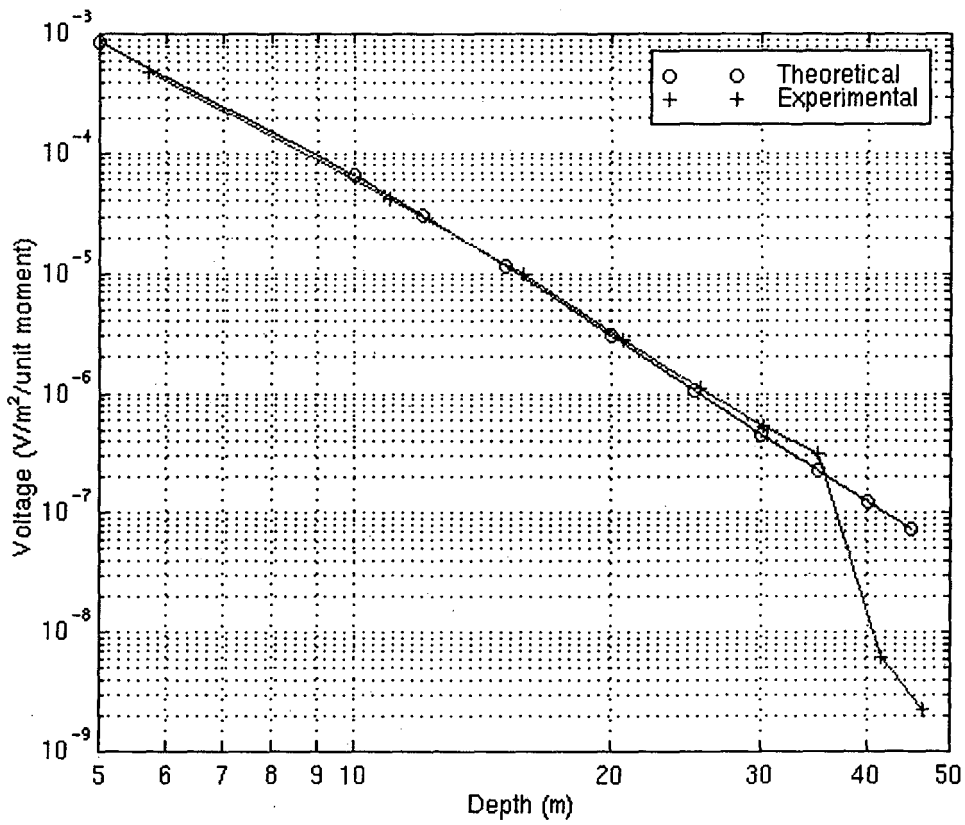Transmitter at 20m

Figure 8 – Determination of transmitter moment

ERNEST ORLANDO LAWRENCE BERKELEY NATIONAL LABORATORY
ONE CYCLOTRON ROAD ¦ BERKELEY, CALIFORNIA 94720